Supplementary material: Assessing the drivers behind the structure and diversity of fish assemblages associated with rocky shores in the Galapagos archipelago

Stijn Bruneel[1,2,*], Wout Van Echelpoel[1], Long Ho[1], Heleen Raat[1], Amber Schoeters[1], Niels De Troyer[1], Ratha Sor[1,3], José Ponton-Cevallos[1,4,5], Ruth Vandeputte[1], Christine Van der heyden[6], Nancy De Saeyer[1], Marie Anne Eurie Forio[1], Rafael Bermudez[5,7], Luis Dominguez-Granda[8], Stijn Luca[9], Tom Moens[2], Peter Goethals[1]

[1]*Department of Animal Sciences and Aquatic Ecology, Ghent University, Coupure Links 653, 9000 Ghent, Belgium,*

[2]*Marine Biology Research Group, Ghent University, Krijgslaan 281, 9000 Ghent, Belgium,*

[3]*Dean of Graduate School, Chea Sim University of Kamchaymear, No. 157, Preah Norodom Blvd, Phnom Penh, Cambodia,*

[4]*Facultad de Ciencias de la Vida, Escuela Superior Politécnica del Litoral (ESPOL), Campus Gustavo Galindo, 09-01-5863 Guayaquil, Ecuador,*

[5]*Galapagos Marine Research and Exploration, GMaRE. Joint ESPOL-CDF program, Charles Darwin Research Station, 200102 Galapagos Islands, Ecuador,*

[6]*University of Applied Sciences and Arts, Valentin Vaerwyckweg 1, 9000 Ghent, Belgium,*

[7]*Facultad de Ingeniería Marítima y Ciencias del Mar, Escuela Superior Politécnica del Litoral (ESPOL), Campus Gustavo Galindo, 09-01-5863 Guayaquil, Ecuador,*

[8]*Centro del Agua y Desarrollo Sustentable, Facultad de Ciencias Naturales y Matemáticas, Escuela Superior Politécnica del Litoral (ESPOL), Campus Gustavo Galindo, 09-01-5863. Guayaquil, Ecuador,*

[9]*Department of Data Analysis and Mathematical Modelling, Ghent University, Coupure Links 653, 9000 Ghent, Belgium*

[*]*To whom correspondence should be addressed; E-mail: stijn.bruneel@ugent.be*

1. Sampling design and data processing and modelling roadmap

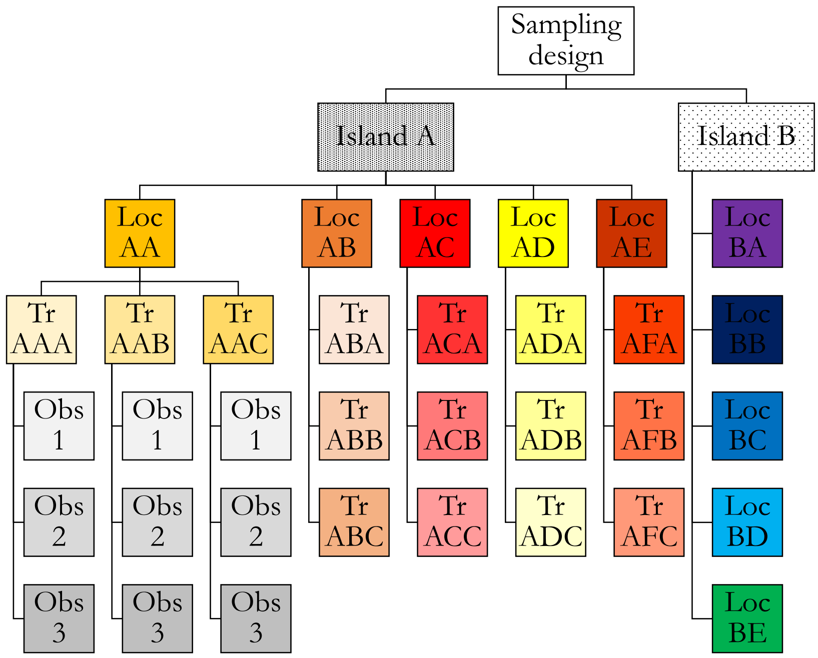

Figure S1.1: Sampling design of the study. Three spatial nested levels can be identified: Island, Location (Loc) and Transect (Tr). Each observer (Obs) covered each transect six times. For clarity reasons, not all subdivisions are presented in this figure. All transects of the different locations of island A were covered by the three observers and the locations of island B were further subdivided in transects, each covered by all three observers. The sampling design was balanced.

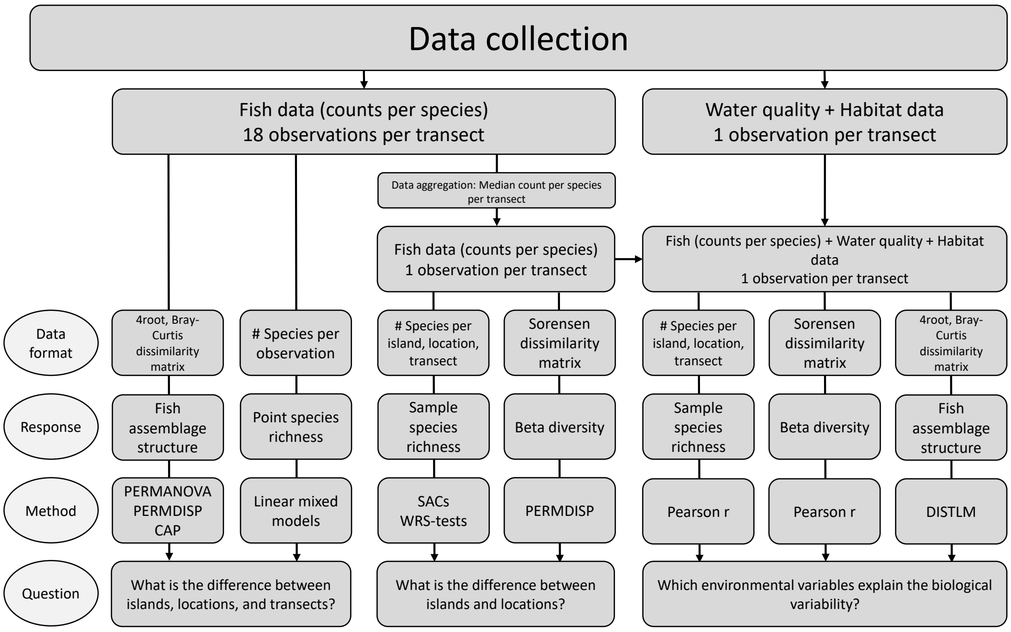

Figure S1.2: Data processing and modelling roadmap used in this study. Fish data and environmental data were collected. For some analyses data was aggregated. The data format, response variable, modelling method and research question of each analysis are depicted. 4root = fourth-root transformed; SAC = Species Accumulation Curves; WRS-tests = Wilcoxon Rank Sum tests.

2. Independence of observations

2.1. Material and Methods

Although not of direct interest in this study, the level of temporal dependence among subsequent observations is important to consider when selecting statistical techniques. As each sampling unit, i.e. transect, was covered multiple times per day, temporal dependence might be an issue as it might obscure other patterns of interest. The level of independence of the observed structure of fish assemblages was assessed using a partial Mantel correlogram (Legendre and Legendre, 2012). The correlation between (1) the number of repeats between observations and (2) the Bray-Curtis dissimilarity values of the fish assemblages was determined while partialling out the effect the sampling unit itself might have had (categorical variable included as matrix of dummy variables). A similar approach was applied to determine the level of independence of the point species richness. The residuals of a simple linear model with as response the point species richness and as predictor the categorical factor Transect was used to estimate the auto-correlation functions (ACF; $r_{k,j}$) of the 18 successive observations ($Y_{1,j}$, $Y_{2,j}$, ..., $Y_{18,j}$) per transect j,

$$\overline{r_{k,j}} = \frac{\sum_{i=1}^{18-k}(Y_{i,j} - \overline{Y_j})(Y_{i+k,j} - \overline{Y_j})}{\sum_{i=1}^{18}(Y_{i,j} - \overline{Y_j})^2} \tag{1}$$

In addition, for each observation lag k, the average ACF over the transects was determined, providing detailed information on the temporal scale at which repeated observations exhibited interdependence. The ecodist and

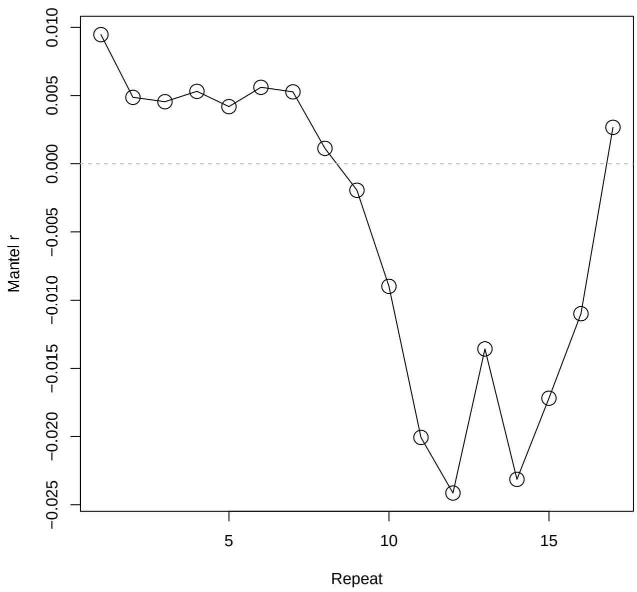

Figure S2.1: Partial mantel correlogram for temporal auto-correlation of the observed structure of fish assemblages. The effect of the sampling units themselves was partialled out. No significant temporal auto-correlations were found.

forest R-packages were used to obtain the partial Mantel correlogram and autocorrelation functions respectively.

2.2. Results and discussion

No significant temporal auto-correlations were found for either the structure of the fish assemblages (Fig. S2.1) or the point species richness (Table S2.1). Hence, the observations could be considered as independent.

lag	1	2	3	4	5	6	7	8	9	10	11	12
ACF	1.00	0.12	0.07	-0.02	-0.06	-0.11	-0.03	-0.12	-0.09	-0.05	-0.02	-0.04

Table S2.1: Averaged temporal auto-correlation function (ACF) of residuals of model with as response point species richness and factor Transect for observation lags from 0 to 12. Auto-correlations were determined per transect and averaged afterwards. No significant temporal auto-correlations were found.

3. Remote sensing

3.1. Material and methods

Environmental data and simulations were collected and processed using the Google Earth Engine (GEE) to study patterns in sea surface temperature (SST), salinity, water velocity and chlorophyll a over a large spatial scale.

SST, salinity and water velocity simulations from the Hybrid Coordinate Ocean Model (HYCOM), which is a data-assimilative hybrid isopycnal-sigma-pressure (generalized) coordinate ocean model (Schaeffer et al., 2008; Cummings and Smedstad, 2013), were provided by the National Ocean Partnership Program (NOPP). The model was run at a temporal resolution of one day and a spatial resolution of 0.08 arc degrees, which corresponds with a grid mesh of 8.85 km latitude and 8.91 km longitude at 0° latitude. Simulations at depths of 0, 10, 50 and 100 meter were performed. Per depth, simulations for the period from 19 August 2017 to 31 August 2017 were aggregated over time per pixel using the median pixel value. A square-shaped normalized boolean kernel was used as a smoother for the pixels. Missing data is depicted as white pixels.

Chlorophyll a data from the MODIS Aqua was provided by NASA (2019). The temporal resolution is two days and the spatial resolution is 0.5 km. Data for the period from 19 August 2017 to 31 August 2017 was aggregated over time per pixel using the median pixel value. Cloud cover was removed from the imagery, causing relatively large gaps in the dataset due to consistent cloud coverage during the study period. Therefore, additional imagery was requested from 1 August 2017 to 15 September 2017 and from 1 June 2017 to 31 August 2017 to have imagery with less and no gaps respectively. A map was constructed with combinations from all three periods. Priority was given to the map of the study period. Empty pixels were first filled up with the 1.5 month series and finally remaining empty pixels were filled up with the 3 month series. A square-shaped normalized boolean kernel was used as a smoother for the pixels of the study period map. Missing data is depicted as white pixels.

3.2. Identification of natural upwelling zones

The presence of the Eastward Equatorial Undercurrent (EUC) or Cromwell current in the Galapagos archipelago is apparent from the different maps. At the surface, water flows mainly in Westward direction due to the presence of the South Equatorial Current (SEC), while at a depth of 100 meter, the water flows mainly in an Eastward direction due to the presence of the EUC. The EUC hits the islands and brings cold, saline, nutrient rich water to the surface through upwelling. The EUC is considered as the main source of nutrients in the Galapagos (Palacios, 2004). From the populated islands, the west of Isabela is clearly the most important upwelling zone, with low temperatures, high salinity and high chlorophyll a concentrations. The Southwest coast of Floreana seems to be another important upwelling zone in terms of temperature and salinity, although chlorophyll a concentrations seem relatively low. The chlorophyll a concentrations seem higher at the Northwest coast of Floreana, which might be the result of the Northward current pushing the nutrients into warmer surface waters, enabling higher productivities of phytoplankton. The upwelling zone on the Southern side of San Cristobal originates from a Northward current, bringing along the waters from the EUC after it is deflected South of Isabela (Liu et al., 2013). EUC waters being deflected to the North seem to be responsible for upwelling in Santiago and the North of Santa Cruz, while the Southern deflection of the EUC causes upwelling in Floreana, San Cristobal and South Santa Cruz. These identified upwelling zones seem similar to the ones described by Schaeffer et al. (2008) for June/July 2006. Although productivity zones in the Galapagos are highly variable (Schaeffer et al., 2008) and climate change has been found to affect local oceanographic variability (Liu et al., 2013), similar sampling periods and comparable intensities of El Niño–Southern Oscillation (ENSO) events should yield similar zones of upwelling. In both July 2006 and August 2017, 3-Month Mean Oceanic Niño Index (ONI) values were very low from March onwards (absolute value below 0.4) and before March only a weak La Niña event was documented (NOAA, 2019). In periods with strong El Niño events, the strength of the EUC diminishes and nutrient supplies go down drastically. For example, the El Niño events of 1982-1983 and 1997-1998 had devastating effects on marine life (Chavez et al., 1999). Hence, the large number of identified upwelling zones indicates the importance of the EUC during this period of the year (Liu et al., 2014).

3.3. Anthropogenic effects or natural upwelling?

During the study period, Floreana was likely affected by upwelling and this was confirmed by the relatively low temperature and salinity found in situ. Furthermore, both Houvenaghel (1978) and Schaeffer et al. (2008) identified an upwelling zone in the southwest coast of Floreana. Schaeffer et al. (2008) described upwelling events in the south coast of Santa Cruz with a strong temporal variability, while Houvenaghel (1978) found no evidence for an upwelling zone around Puerto Ayora. During the study period, some upwelling west of Puerto Ayora was apparent from remote sensing imagery, although in situ measurements of temperature and salinity were respectively significantly higher and lower in Puerto Ayora than in Floreana. The high temperature and low salinity in Puerto Ayora did not suggest the presence of an upwelling zone, although the waters reaching the bay could have been recently upwelled waters which originated westward of Puerto Ayora. The higher temperature and lower salinity in Puerto Ayora could have been the result of solar heating, resulting in increased productivity explaining the relatively high in situ chlorophyll concentrations (Houvenaghel, 1978). Similarly, the spatial mismatch between high chlorophyll concentrations and observed zones of upwelling of the satellite imagery, could have been the result of the lower temperatures of the upwelling zones, limiting productivity. For example, while upwelling was apparent on the southwest coast of Floreana, high phytoplankton biomass production was only apparent north of this zone, where temperature was generally higher. In Puerto

Ayora, the supply of nutrients from nearby upwelling in combination with the higher temperature explain the higher productivity, but not the high nutrient concentrations which were expected to be lower than for Floreana because of the clear upwelling in the latter. The high nutrient concentrations in Puerto Ayora, might have been the result of replenishing through local upwelling at a finer temporal and/or spatial scale than could be measured and observed with the in situ measurements, available models and satellite imagery. However, it is more likely that the coastal waters have been enriched with nutrients from anthropogenic origin, as has already been suggested in other studies (Werdeman, 2006; Mateus et al., 2019).

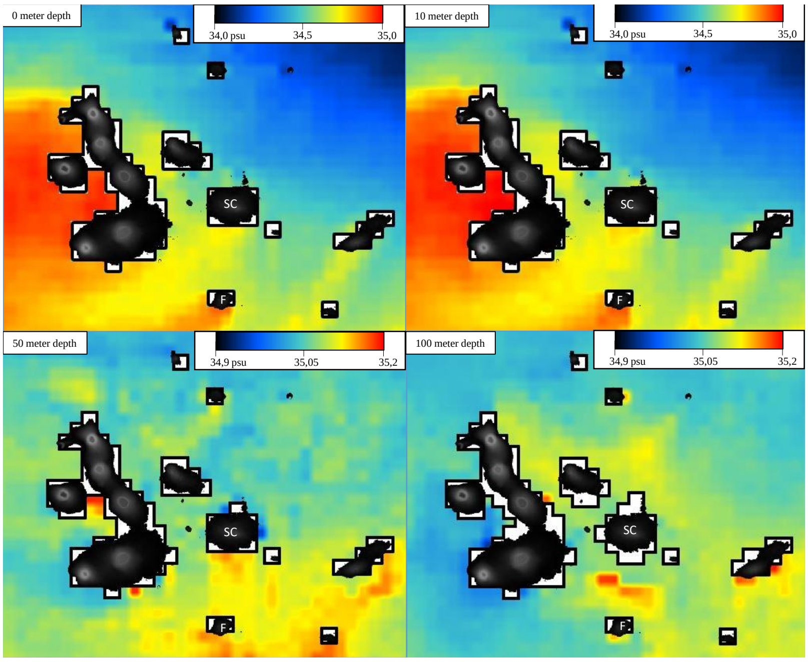

Figure S3.1: Sea water salinity, in practical salinity units (psu), at depths of 0, 10, 50 and 100 meter. The data were obtained from HYCOM simulations. The islands of Santa Cruz (SC) and Floreana (F) are indicated.

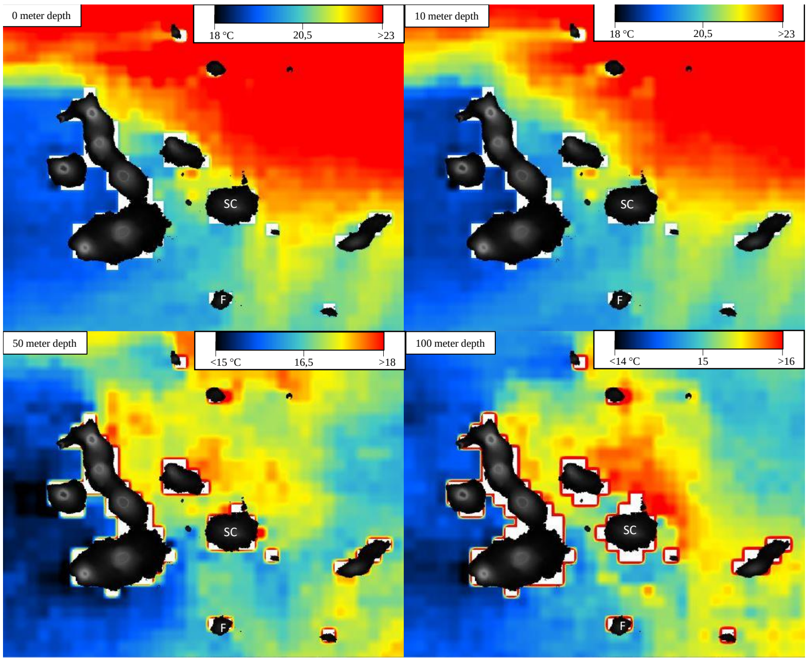

Figure S3.2: Sea surface temperature, in °C, at depths of 0, 10, 50 and 100 meter. The data were obtained from HYCOM simulations. The islands of Santa Cruz (SC) and Floreana (F) are indicated. The color scale of the map of 100 meter is different from the color scales of the other maps.

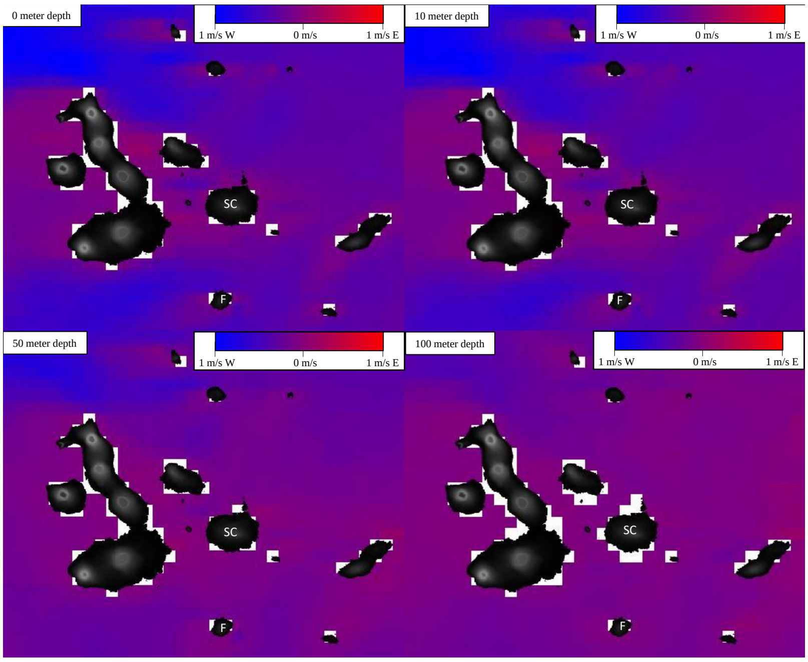

Figure S3.3: Eastward water velocity, in m s^{-1} Eastward (E) and m s^{-1} Westward (W), at depths of 0, 10, 50 and 100 meter. The data were obtained from HYCOM simulations. The islands of Santa Cruz (SC) and Floreana (F) are indicated.

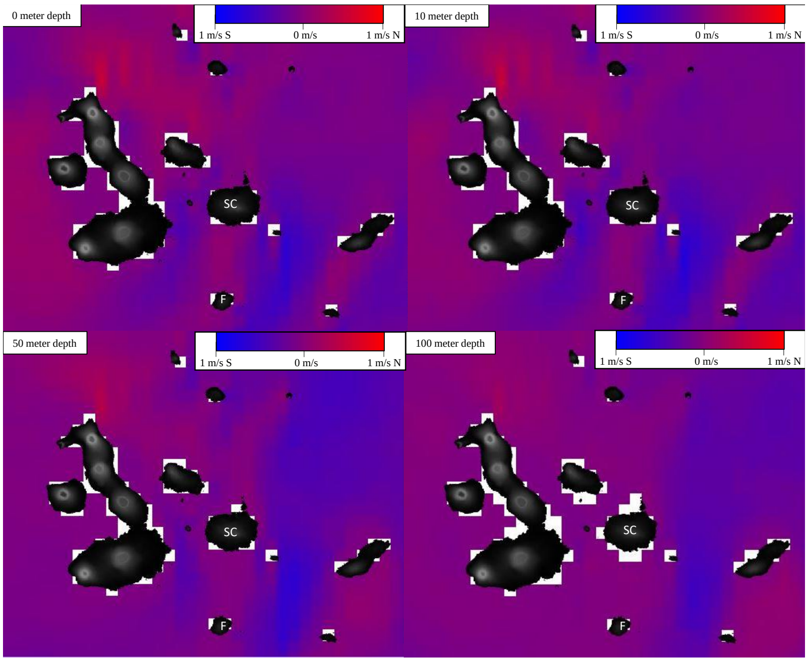

Figure S3.4: Northward water velocity, in m s^{-1} Northward (N) and m s^{-1} Southward (S), at depths of 0, 10, 50 and 100 meter. The data were obtained from HYCOM simulations. The islands of Santa Cruz (SC) and Floreana (F) are indicated.

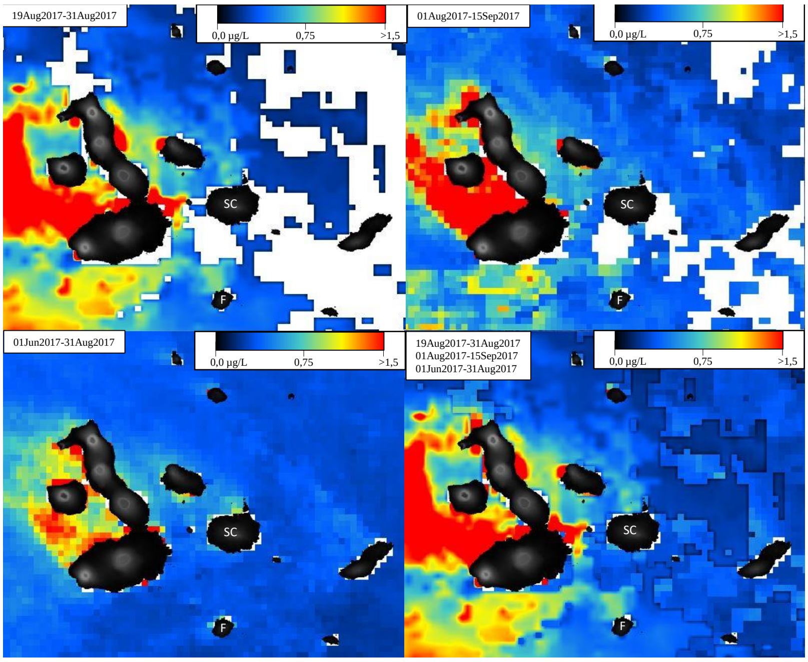

Figure S3.5: Chlorophyll a concentration, in µg L^{-1}, at a depth of 0 meter, for the period 19 August 2017 to 31 August 2017, 1 August 2017 to 15 September 2017 and 1 June 2017 to 31 August 2017. A combination map was constructed with priority given to the shorter periods. The data were obtained from MODIS Aqua. The islands of Santa Cruz (SC) and Floreana (F) are indicated.

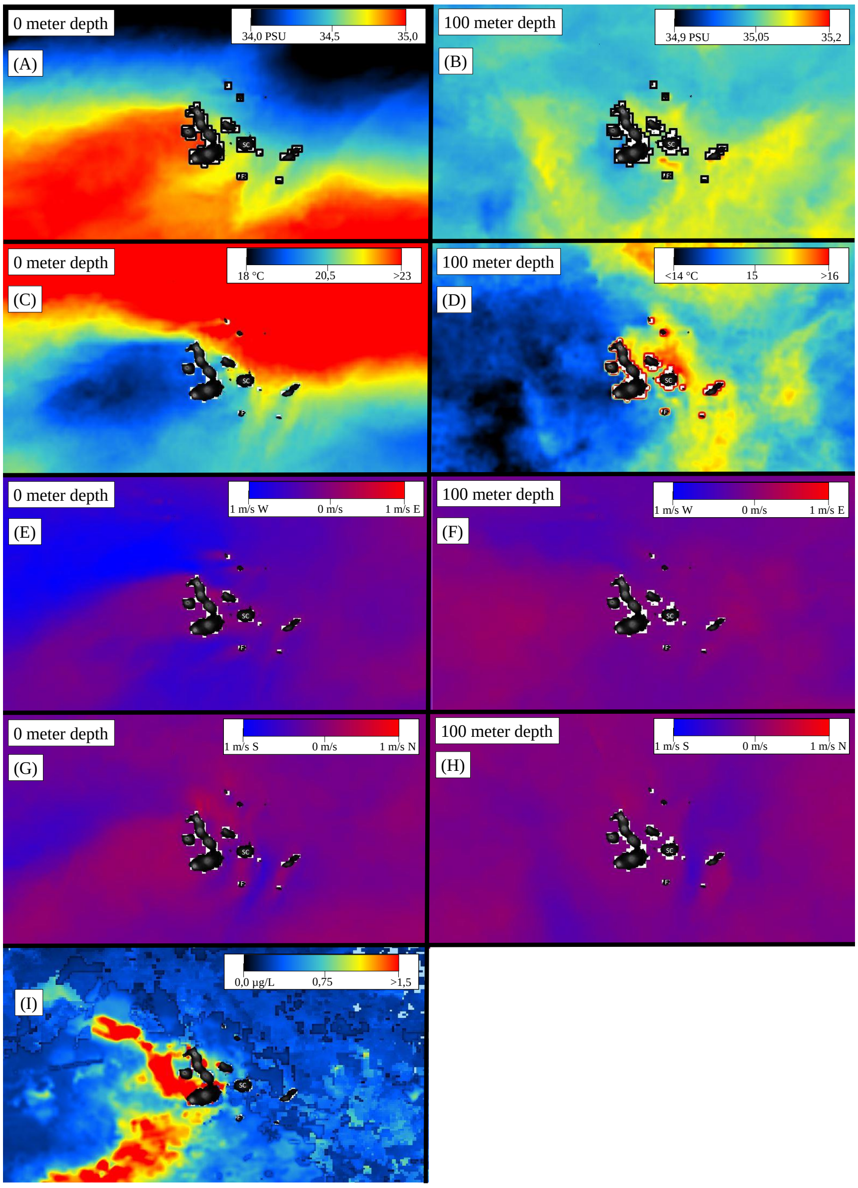

Figure S3.6: Sea water salinity (A and B), in practical salinity units (psu), sea surface temperature (C and D), in °C, Eastward water velocity (E and F), in m s^{-1} Eastward (E) and m s^{-1} Westward (W) and Northward water velocity (G and H), in m s^{-1} Northward (N) and m s^{-1} Southward (S), at depths of 0 and 100 meter. Chlorophyll a concentration (I), in µg L^{-1}, at a depth of 0 meter. The islands of Santa Cruz (SC) and Floreana (F) are indicated.

4. Environmental analyses

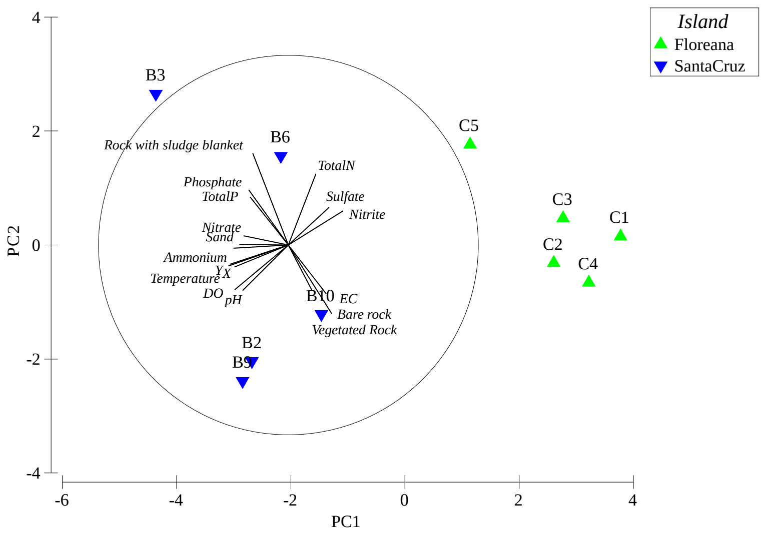

Figure S4.1: Principal component analysis (PCA) of locations at Floreana and Santa Cruz island based on the water variables, physical habitats and geographical distance. PC1 and PC2 explained 53.3 % and 16.1 % of the variation, respectively.

Variable	Floreana				Santa Cruz			
	mean	sd	min	max	mean	sd	min	max
Nitrite (mg N L^{-1})*	0.02	0.01	0.01	0.03	0.01	0.00	0.00	0.01
Nitrate (mg N L^{-1})	0.32	0.14	0.22	0.56	0.48	0.07	0.40	0.59
Ammonium (mg N L^{-1})*	0.01	0.00	0.01	0.01	0.02	0.01	0.00	0.04
Sulfate (mg L^{-1})*	1.42	0.07	1.31	1.47	0.99	0.48	0.13	1.26
TotalN (mg N L^{-1})	0.76	0.21	0.48	1.04	0.56	0.14	0.36	0.73
Phosphate (mg P L^{-1})	0.04	0.02	0.02	0.06	0.06	0.04	0.03	0.13
TotalP (mg P L^{-1})	0.09	0.12	0.02	0.31	0.11	0.04	0.08	0.17
DO (mg L^{-1})*	8.84	0.58	8.21	9.43	11.16	1.78	9.50	13.95
EC (mS cm^{-1})	49.56	4.84	41.90	53.00	46.18	3.99	42.10	52.50
Temperature (°C)*	19.30	0.96	18.20	20.40	23.30	1.20	22.20	25.20
pH (-)*	7.98	0.08	7.90	8.07	8.29	0.13	8.20	8.51
Chlorophyll (µg L^{-1})	4.31	5.94	0.00	13.20	10.29	4.31	3.50	15.58
Sand (%)*	9.00	9.00	0.00	23.00	25.00	6.00	18.00	32.00
Vegetated rock (%)	68.00	16.00	39.00	81.00	40.00	29.00	0.00	82.00
Rock with sediment deposition (%)	5.00	12.00	0.00	27.00	26.00	34.00	0.00	75.00
Bare rock (%)	18.00	8.00	10.00	28.00	9.00	13.00	0.00	27.00

Table S4.1: Water conditions and percentage cover of physical habitats of the assessed locations of Santa Cruz and Floreana island. The mean, standard deviation (sd), minimum (min) and maximum (max) for each island are given. Variables with significant differences between the islands ($p<0.05$; Wilcoxon rank sum test) are indicated with *.

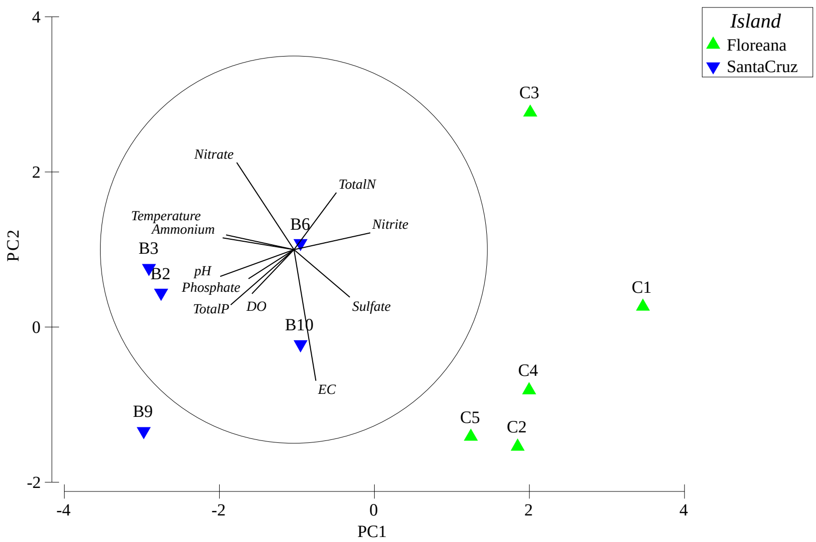

Figure S4.2: Principal component analysis (PCA) of locations at Floreana and Santa Cruz island based on the water parameters. PC1 and PC2 explained 52.2 % and 16.7 % of the variation, respectively.

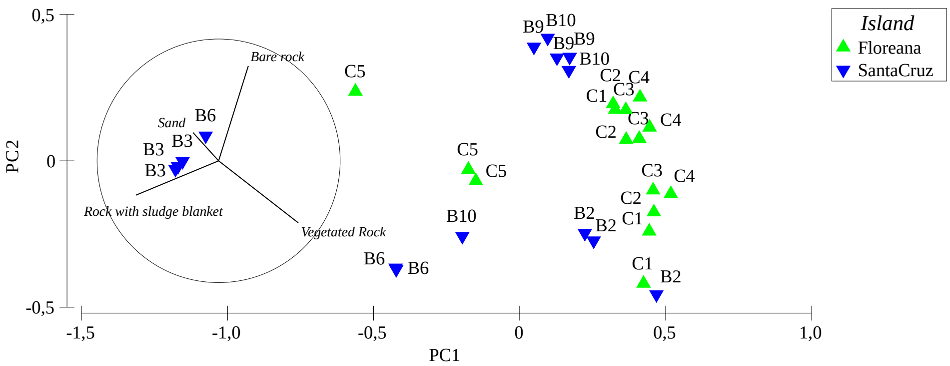

Figure S4.3: Principal component analysis (PCA) of transects at Floreana and Santa Cruz island based on the physical habitats. PC1 and PC2 explained 74.2 % and 16.4 % of the variation, respectively. Per location there were 3 transects (n=30).

Island	Location	Subsample	Coliforms	*E. Coli*
Floreana	C1	I	X	X
	C2	I	X	
	C3	I		
	C4	I		
	C5	I	X	
Santa Cruz	B2	I	X	X
		II	X	X
		III	X	X
	B4	I	X	X
		II	X	X
		III	X	X
	B10	I	X	X
		II	X	X
		III	X	X

Table S4.2: Presence/absence of coliforms and *E. Coli* at different locations of Santa Cruz and Floreana island. Presences are indicated as X.

5. Fish α and β diversity

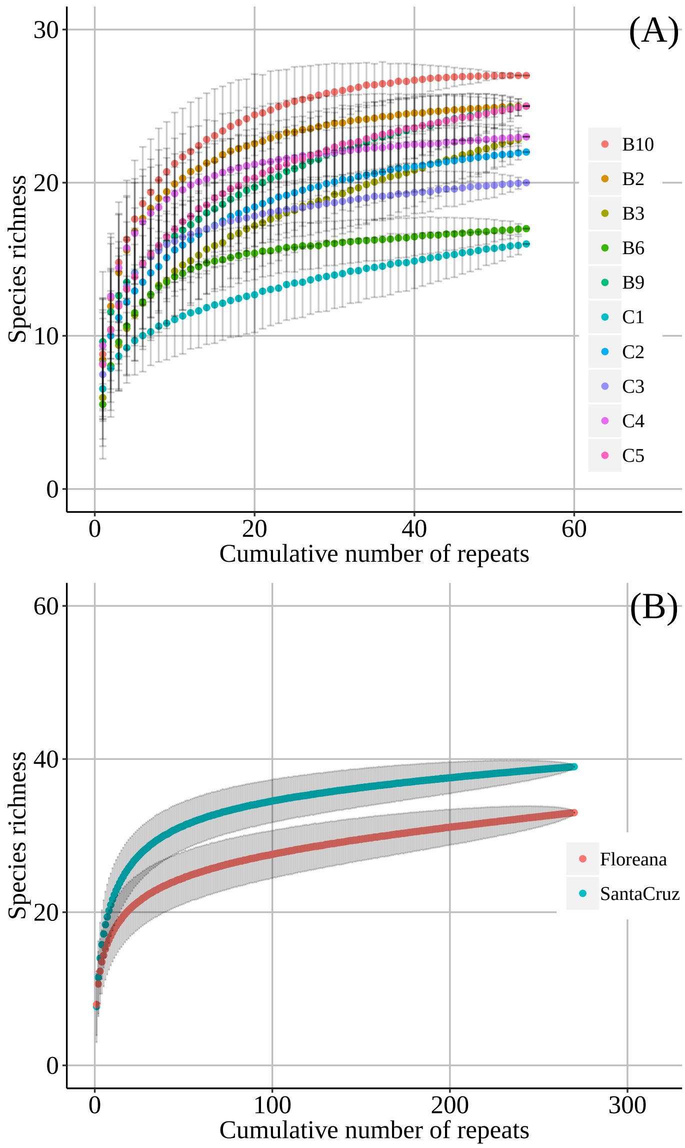

Figure S5.1: Species Accumulation Curves (SACs) of the different locations (A) and islands (B). 10000 permutations were used for each cumulative number of observations to construct the graphs. The error bars correspond with the 95 % confidence interval.

Range	Species	Floreana					Santa Cruz				
		C1	C2	C3	C4	C5	B10	B2	B3	B6	B9
Endemic	Black striped salema *Xenocys jessiae*	2.78 (11.56)	0	0	155.67 (239.08)	6.19 (32.17)	22.76 (36.11)	0	0	0	0
	Bravo clinid *Gobioclinus dendriticus*	5.22 (3.64)	1.85 (1.56)	1.09 (1.52)	0.98 (1.32)	4.43 (3.48)	0.19 (0.48)	0.39 (0.56)	0.52 (1.45)	0.41 (0.79)	0.56 (0.96)
	Galapagos grunt *Orthopristis forbesi*	0	0	0	0	0	0.04 (0.19)	0	0.07 (0.33)	4.17 (12.43)	0
	Galapagos Seabream *Archosargus pourtalesi*	0	0	0	0	0	2.63 (5.59)	1.98 (3.82)	0	0	0
	Galapagos triplefin blenny *Lepidonectes corallicola*	0.07 (0.33)	0	0.13 (0.34)	0.41 (0.71)	0.06 (0.23)	0	0	0	0.02 (0.14)	0
	Marbled goby *Gobio manchada*	0.07 (0.33)	0.07 (0.26)	0.72 (1.02)	1.61 (1.77)	0.46 (1.09)	0.26 (0.56)	0.04 (0.19)	11.7 (19.14)	1.63 (2.10)	1.74 (2.17)
	Triplefin blenny *Lepidonectes corallicola*	0	0.02 (0.14)	0	0	0	0	0	0	0	0
	White salema *Xenichthys agassizii*	0	0	0	1.11 (8.16)	3.24 (10.71)	86.35 (126.2)	0	0.91 (2.53)	1.11 (3.60)	0.06 (0.41)
Indo-Pacific	Balloon fish *Diodon holocanthus*	0	0	0.02 (0.14)	0	0	0	0	0	0	0
	Blue chin parrotfish *Scarus ghobban*	0	0.54 (2.10)	0.02 (0.14)	0	0	1.02 (2.73)	0	0	0	0.04 (0.19)
	Bullseye puffer *Sphoeroides annulatus*	0	0.02 (0.14)	0	0	0.02 (0.14)	1.48 (1.59)	0.39 (0.74)	4.17 (3.47)	0.80 (1.25)	0.04 (0.19)
	Eagle ray *Aetobatus narinari*	0	0	0	0	0	0	0	0	0	0.02 (0.14)
	Galapagos shark *Carcharhinus galapagensis*	0	0	0	0	0	0.04 (0.19)	0.02 (0.14)	0	0	0
	Jewel moray *Muraena lentiginosa*	0	0	0	0	0.02 (0.14)	0.07 (0.33)	0.04 (0.19)	0	0	0.04 (0.19)
	Pacific spotfin mojarra *Eucinostomus dowii*	0	0	0	0	0	13.59 (12.86)	2.59 (6.22)	2.06 (2.33)	2.98 (3.75)	20.46 (12.22)
	Reef cornetfish *Fistularia commersonii*	0	0	0	0	0.11 (0.50)	0.39 (0.74)	0.07 (0.26)	0	0	0
	Spotted cabrilla *Epinephelus analogus*	0	0	0	0	0	0	0	0.02 (0.14)	0	0
	Wounded wrasse *Halichoeres chierchiae*	0	0	0	0	0	0.13 (0.52)	1.04 (2.53)	0.02 (0.14)	0.02 (0.14)	0.57 (1.51)
Panamic	Blacktip cardinalfish *Apogon atradorsatus*	1.39 (10.21)	182.11 (282.62)	28.98 (45.51)	58.70 (114.14)	8.80 (14.95)	0	1.44 (2.35)	0	0	0.07 (0.33)
	Blue and gold snapper *Lutjanus viridis*	0.02 (0.14)	0.04 (0.19)	2.67 (5.64)	0.06 (0.23)	0.09 (0.29)	0	0	0	0	0
	Cortez rainbow wrasse *Thalassoma lucasanum*	18.28 (13.22)	12.78 (10.56)	10.59 (7.43)	15.52 (9.1)	6.00 (4.16)	0.65 (1.08)	24.89 (24.76)	0.70 (1.22)	0.94 (1.71)	9.02 (6.48)
	Galapagos ringtail damselfish *Stegastes beebei*	55.91 (14.82)	31.98 (18.82)	11.52 (8.09)	8.98 (6.24)	26.46 (18.8)	3.31 (4.65)	0.74 (1.05)	0	0.67 (1.03)	5.11 (3.08)
	Giant hawkfish *Cirrhitus rivulatus*	0	0.17 (0.50)	0.04 (0.19)	0.11 (0.37)	0	0	0.07 (0.26)	0	0	0.04 (0.19)
	Mojarra grunt *Haemulon scudderii*	0	0	0	0	0	0.04 (0.19)	0	0.02 (0.14)	0.15 (0.60)	0
	Mullet snapper *Lutjanus aratus*	0	0	0	0	0	0	0	0	0	0.06 (0.30)
	Pacific dog snapper *Lutjanus novemfasciatus*	0	0	0	0	0	0	0	0	0.19 (0.68)	0
	Razor surgeonfish *Prionurus laticlavius*	0	9.11 (19.79)	0.59 (1.64)	0.37 (0.71)	1.61 (3.58)	0	0.35 (1.23)	0.02 (0.14)	0	0
	Spinster wrasse *Halichoeres nicholsi*	0.30 (0.66)	1.76 (1.44)	1.50 (1.59)	4.65 (3.75)	2.06 (2.92)	5.87 (6.27)	8.17 (13.28)	0.13 (0.44)	0	15.80 (6.78)
	Stone scorpionfish *Scorpaena mystes*	0	0.04 (0.19)	0	0.13 (0.34)	0	0	0	0	0	0
	Yellowtail damselfish *Microspathodon bairdii*	1.07 (1.16)	12.83 (68.14)	1.24 (2.78)	1.57 (1.92)	7.07 (8.85)	131.15 (31.03)	138.83 (39.24)	167.7 (50.4)	23.28 (14.95)	318.76 (80.68)
Peruvian	Galapagos bullhead shark *Heterodontus quoyi*	0	0	0	0	0.02 (0.14)	0	0	0	0	0
	Galapagos sheepshead wrasse *Semicossyphus darwini*	0	0	0	0	0	0	0	0	0	0.06 (0.41)
	Harlequin wrasse *Bodianus eclancheri*	0	0	0	0	0.07 (0.26)	0	0	0	0	0
Widespread	Amarillo snapper *Lutjanus argentiventris*	0	0	0	0	0	0.09 (0.29)	0	0.22 (0.46)	0.20 (0.53)	0
	Banded wrasse *Halichoeres notospilus*	0.02 (0.14)	0.07 (0.26)	0.30 (0.86)	0.30 (0.72)	0.19 (0.65)	0.11 (0.46)	3.46 (5.09)	0.61 (1.12)	0	1.19 (1.85)
	Chameleon wrasse *Halichoeres dispilus*	23.06 (14.29)	57.78 (26.00)	26.52 (12.9)	21.69 (12.9)	62.8 (47.23)	2.93 (4.09)	0.61 (1.63)	0	0	2.30 (2.57)
	Flag cabrilla *Epinephelus labriformis*	0	0.09 (0.35)	0.09 (0.29)	0.19 (0.44)	0.04 (0.19)	0.06 (0.23)	0.04 (0.19)	0	0	0.17 (0.42)
	King angelfish *Holacanthus passer*	0.02 (0.14)	0.06 (0.23)	0.04 (0.19)	0.09 (0.29)	0.06 (0.23)	0	0	0	0	0
	Loosetooth parrotfish *Nicholsina denticulata*	0	0	0	0.02 (0.14)	0	0	0	0	0	0
	Marbled ray *Taeniurops meyeni*	0	0	0	0	0	0	0	0.02 (0.14)	0	0
	Mexican hogfish *Bodianus diplotaenia*	0.37 (0.56)	0.31 (0.80)	0.69 (0.99)	0.31 (0.54)	0.78 (1.44)	0.06 (0.30)	0.11 (0.37)	0.02 (0.14)	0	0
	Panamic fanged blenny *Ophioblennius steindachneri*	0.61 (0.86)	0.28 (0.60)	0.39 (0.63)	3.00 (2.37)	0.02 (0.14)	0.07 (0.26)	1.24 (1.16)	0.17 (0.38)	0.17 (0.47)	0.02 (0.14)
	Panamic sergeant major *Abudefduf troschelii*	0	0.04 (0.27)	0	0	0	2.89 (7.44)	24.87 (26.7)	23.54 (19.56)	8.91 (7.69)	112.50 (76.73)
	Sabertooth blenny *Plagiotremus azaleus*	1.74 (1.78)	2.67 (3.48)	1.91 (2.35)	1.44 (1.73)	2.63 (3.07)	0.31 (0.67)	3.02 (3.42)	0.02 (0.14)	0	2.33 (2.08)
	Striped mullet *Mugil cephalus*	0	0	0	0	0.28 (2.04)	0	0	0	0	0
	Three banded butterfly fish *Chaetodon humeralis*	0	0	0	0	0	1.43 (1.62)	0.17 (0.47)	0.02 (0.14)	0.26 (0.65)	0.06 (0.30)
	Throat-spotted blenny *Malacoctenus tetranemus*	0	0	0	0.09 (0.29)	0	0	0	0	0	0
	Tiger snake eel *Myrichthys maculosus*	0	0	0	0	0	0	0.11 (0.42)	0.19 (0.44)	0	0.07 (0.26)
	White mullet *Mugil curema*	0	0	0	0	0	0	0	0.37 (1.95)	0	0

Table S5.1: List of species observed during the study for each location. Mean (and standard deviation) per location are given. The classification of geographical ranges used in the study of Edgar et al. (2004) were adopted. The FishBase (fishbase.org) was used to determine the range of each species.

Variable	Both islands (Location) Sample	Both islands (Location) Point	Floreana (Location) Sample	Floreana (Location) Point	Santa Cruz (Location) Sample	Santa Cruz (Location) Point
Nitrite (mg N L^{-1})	-0.64*	-0.30	-0.96*	-0.82	-0.44	-0.32
Nitrate (mg N L^{-1})	0.12	-0.16	0.03	0.00	-0.56	-0.68
Ammonium (mg N L^{-1})	0.17	-0.09	0.00	0.00	-0.18	-0.17
Sulfate (mg L^{-1})	-0.21	0.05	0.59	0.65	-0.13	-0.01
TotalN (mg N L^{-1})	-0.44	-0.37	0.00	-0.29	-0.68	-0.54
Phosphate (mg P L^{-1})	0.22	-0.31	0.70	0.51	-0.30	-0.71
TotalP (mg P L^{-1})	0.40	-0.14	0.71	0.19	-0.63	-0.94*
DO (mg L^{-1})	0.63*	0.52	0.86	0.87	0.57	0.73
EC (mS cm^{-1})	0.33	0.71*	0.59	0.65	0.47	0.94*
Temperature (°C)	0.52	0.17	0.52	0.09	0.59	0.51
pH (-)	0.53	0.40	0.82	0.74	0.36	0.77
Sand (%)	0.37	-0.02	0.12	-0.48	0.53	0.59
Vegetated Rock (%)	-0.17	0.37	-0.79	-0.27	0.30	0.61
Rock with sediment deposition (%)	-0.07	-0.63	0.62	0.05	-0.62	-0.91*
Bare rock (%)	0.22	0.69*	0.31	0.73	0.59	0.85

	Both islands (Transect) Sample	Both islands (Transect) Point	Floreana (Transect) Sample	Floreana (Transect) Point	Santa Cruz (Transect) Sample	Santa Cruz (Transect) Point
Sand (%)	0.11	0.13	-0.36	-0.21	0.35	0.52*
Vegetated Rock (%)	-0.03	0.15	-0.45	-0.43	0.30	0.42
Rock with sediment deposition (%)	-0.24	-0.50*	0.08	0.05	-0.54*	-0.78*
Bare rock (%)	0.36	0.57*	0.71*	0.65*	0.41	0.65*

Table S5.2: Pearson correlation coefficients of sample species richness (Sample) and point species richness (Point) versus different environmental variables. The sample species richness was defined as the total number of species observed within one location or transects (SAC), while the point species richness was defined as the average number of species over the different observations of a specific location or transect. Significant correlations ($p<0.05$) were indicated with *.

Variable	Both islands	Floreana	Santa Cruz
Nitrite (mg N L^{-1})	-0.02	0.15	0.29
Nitrate (mg N L^{-1})	0.38	0.91*	-0.14
Ammonium (mg N L^{-1})	-0.03	0.00	-0.34
Sulfate (mg L^{-1})	-0.48	-0.79	-0.45
Total N (mg N L^{-1})	0.12	0.81	-0.01
Phosphate (mg P L^{-1})	-0.24	-0.80	-0.20
Total P (mg P L^{-1})	-0.06	-0.49	0.19
DO (mg L^{-1})	-0.42	-0.53	-0.92*
EC (mS cm^{-1})	-0.64*	-0.85	-0.57
Temperature (°C)	0.10	0.56	-0.49
pH (-)	-0.09	-0.06	-0.66
Sand (%))	-0.15	-0.38	-0.88*
Vegetated Rock (%)	0.17	0.23	0.36
Rock with sediment deposition (%)	0.15	-0.27	0.17
Bare rock (%)	-0.52	0.41	-0.68

Table S5.3: Pearson correlation coefficients of beta diversity, determined as distance-to-centroid (Sorensen resemblance matrix), versus different environmental variables. Significant correlations ($p<0.05$) were indicated with *.

Island	Group	β diversity		Physical habitat variability	
		Average	SE	Average	SE
Floreana	C1	11.72	3.10	0.87	0.30
	C2	7.65	2.50	0.51	0.18
	C3	20.80	3.10	0.39	0.12
	C4	13.59	2.90	0.46	0.16
	C5	10.42	3.97	0.75	0.19
Santa Cruz	B10	14.14	4.75	1.13	0.28
	B2	22.56	6.58	0.66	0.17
	B3	9.96	3.74	0.11	0.04
	B6	27.63	4.34	1.31	0.33
	B9	3.82	1.73	0.35	0.14

Table S5.4: Distance-to-centroid for Sorensen resemblance matrix of fish assemblage data per location, representing the β diversity, and distance-to-centroid for the physical habitat data, representing the habitat variability of each location (n=3). Average values and standard errors (SE) are given.

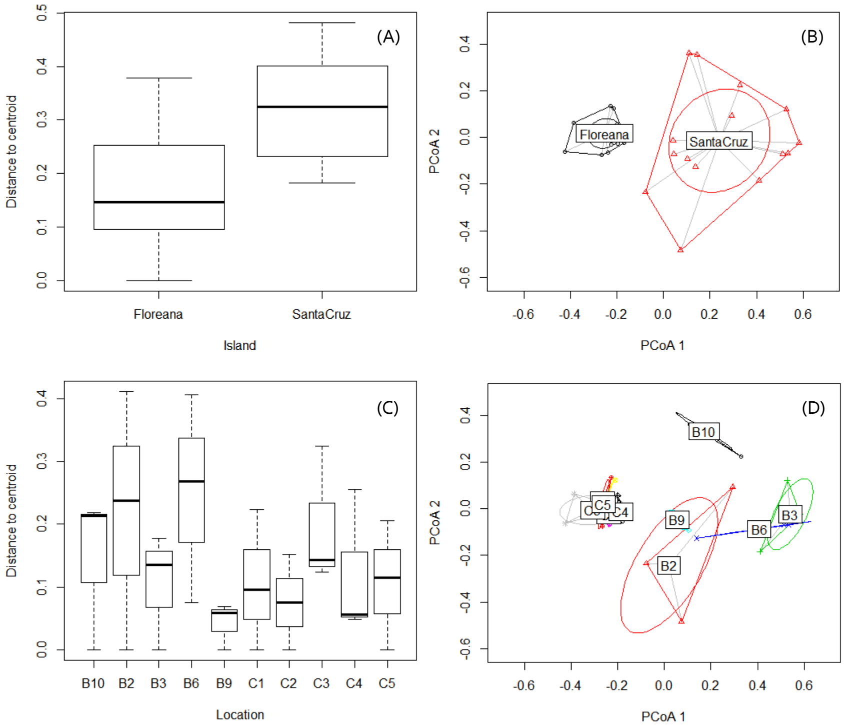

Figure S5.2: β diversity of the different islands (A and B) and locations (C and D). In figures A and C, the distance of each transect to centroid is given per island and per location respectively. In figures B and D, the distance of each transect to the centroid of the concerning island or location is depicted in a PCO plot.

6. PERMANOVA

	Both islands	Santa Cruz	Floreana
σ'_{Island}	39.39**	/	/
$\sigma'_{Observer}$	2.72	1.76	3.86
$\sigma'_{Location}$	18.41**	23.63**	10.94*
$\sigma'_{Island:Observer}$	1.25	/	/
$\sigma'_{Transect}$	18.61**	20.53**	11.26**
$\sigma'_{Location:Observer}$	8.98**	8.65**	9.29**
$\sigma'_{Transect:Observer}$	10.92**	10.56**	11.26**
$\sigma'_{Residuals}$	16.49	17.27	15.68
$\% \ \sigma'^2_{Island}$	57.09	/	/
$\% \ \sigma'^2_{Observer}$	0.27	0.21	2.07
$\% \ \sigma'^2_{Location}$	12.47	38.05	16.62
$\% \ \sigma'^2_{Island:Observer}$	0.06	/	/
$\% \ \sigma'^2_{Transect}$	12.74	28.72	17.60
$\% \ \sigma'^2_{Location:Observer}$	2.97	5.10	11.98
$\% \ \sigma'^2_{Transect:Observer}$	4.39	7.60	17.60
$\% \ \sigma'^2_{Residuals}$	10.01	20.32	34.13

Table S6.1: Square root estimates of components of variation (σ') and the percentage of variation of each component to the total variation of PERMANOVA models based on Bray-Curtis dissimilarities (fourth-root-transformed) with Island and Location as fixed factors, Transect as nested random factor and Observer as crossed random factor. *p<0.05, **p<0.01

7. PCO analysis

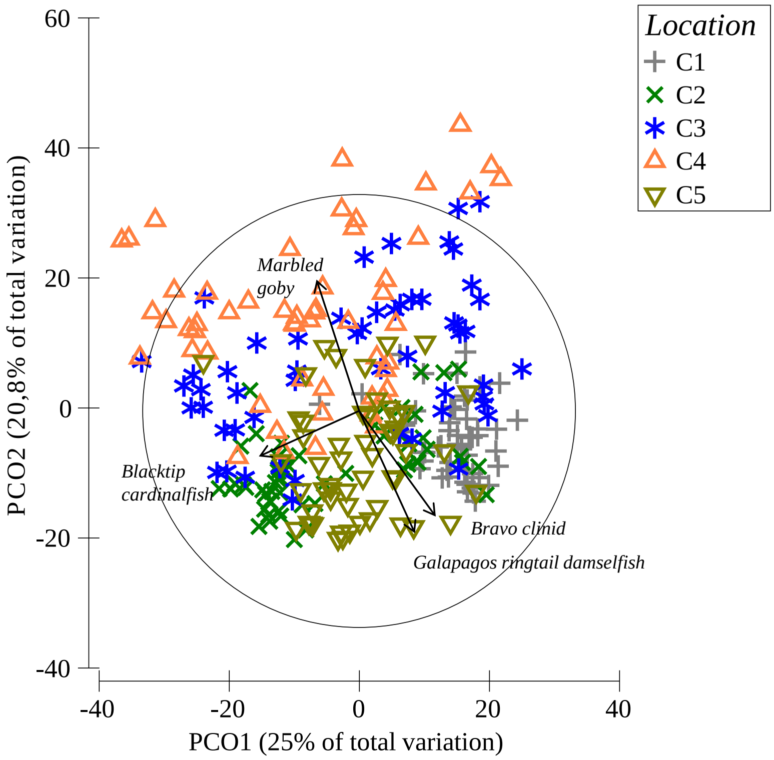

Figure S7.1: PCO based on Bray-Curtis resemblance matrix with distinction of the different locations in Floreana. The fish species with a Pearson correlation of more than 0.5 with the ordination axes are represented as vectors.

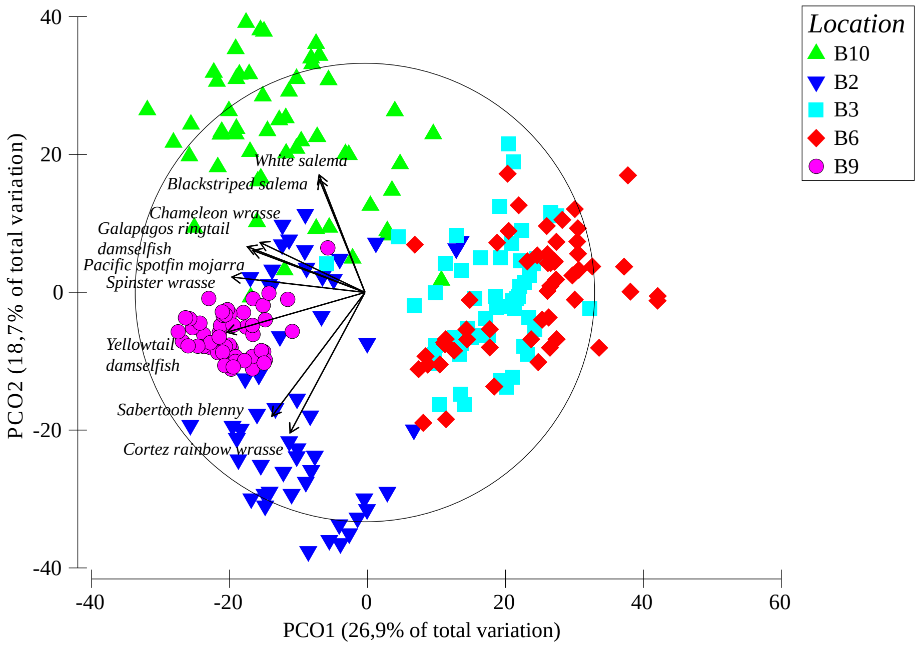

Figure S7.2: PCO based on Bray-Curtis resemblance matrix with distinction of the different locations in Santa Cruz. The fish species with a Pearson correlation of more than 0.5 with the ordination axes are represented as vectors.

8. CAP analysis

Orig. group	Classified B10	B2	B3	B6	B9	Total	% Correct
B10	47	3	1	0	3	54	87.04
B2	1	49	0	2	2	54	90.74
B3	0	1	53	0	0	54	98.15
B6	0	0	4	50	0	54	92.59
B9	1	0	0	0	53	54	98.15

Table S8.1: Classification success (% correct) of CAP leave-one-out cross-validation for locations in Santa Cruz.

Orig. group	Classified C1	C2	C3	C4	C5	Total	% correct
C1	48	2	2	2	0	54	88.89
C2	8	28	3	0	15	54	51.85
C3	8	7	31	7	1	54	57.41
C4	5	3	10	36	0	54	66.67
C5	3	13	9	0	29	54	53.70

Table S8.2: Classification success (% correct) of CAP leave-one-out cross-validation for locations in Floreana.

Orig. group		Classified															Total	% correct
		B10			B2			B3			B6			B9				
		A	B	C	A	B	C	A	B	C	A	B	C	A	B	C		
B10	A	16	2	0	0	0	0	0	0	0	0	0	0	0	0	0	18	88.89
	B	2	11	2	3	0	0	0	0	0	0	0	0	0	0	0	18	61.11
	C	0	5	13	0	0	0	0	0	0	0	0	0	0	0	0	18	72.22
B2	A	0	0	1	15	1	0	0	0	0	0	1	0	0	0	0	18	83.33
	B	0	0	0	0	12	5	0	0	0	0	0	0	0	0	1	18	66.67
	C	0	0	0	0	1	17	0	0	0	0	0	0	0	0	0	18	94.44
B3	A	0	0	0	0	0	0	15	3	0	0	0	0	0	0	0	18	83.33
	B	0	0	0	0	0	0	1	17	0	0	0	0	0	0	0	18	94.44
	C	0	0	0	0	0	0	4	3	11	0	0	0	0	0	0	18	61.11
B6	A	0	0	0	0	0	0	0	0	0	18	0	0	0	0	0	18	100.00
	B	0	0	0	0	0	0	0	0	0	0	17	1	0	0	0	18	94.44
	C	0	0	0	0	0	0	0	1	1	0	2	14	0	0	0	18	77.78
B9	A	0	0	0	0	0	0	0	0	0	0	0	0	10	5	3	18	55.56
	B	0	0	0	0	0	0	0	0	0	0	0	0	6	10	2	18	55.56
	C	0	0	0	0	0	0	0	0	0	0	0	0	7	2	9	18	50.00

Table S8.3: Classification success (% correct) of CAP leave-one-out cross-validation for transects in Santa Cruz.

Orig. group		Classified															Total	%correct
		C1			C2			C3			C4			C5				
		A	B	C	A	B	C	A	B	C	A	B	C	A	B	C		
C1	A	10	4	2	0	1	0	0	0	0	0	1	0	0	0	0	18	55.56
	B	0	16	1	0	0	0	0	1	0	0	0	0	0	0	0	18	88.89
	C	3	2	12	0	0	0	0	0	1	0	0	0	0	0	0	18	66.67
C2	A	0	0	0	8	1	3	0	0	2	0	0	0	1	3	0	18	44.44
	B	1	1	0	0	14	0	0	1	0	0	0	0	1	0	0	18	77.78
	C	0	0	0	1	0	17	0	0	0	0	0	0	0	0	0	18	94,44
C3	A	0	0	1	0	0	0	14	0	0	2	0	0	1	0	0	18	77.78
	B	1	1	0	0	2	4	1	4	1	2	1	1	0	0	0	18	22.22
	C	0	0	0	2	0	1	0	1	10	0	0	3	1	0	0	18	55.56
C4	A	0	0	0	0	1	0	1	2	0	8	5	0	1	0	0	18	44.44
	B	0	0	0	0	1	0	0	2	0	1	9	5	0	0	0	18	50.00
	C	2	0	0	2	0	0	0	0	0	0	0	13	0	1	0	18	72.22
C5	A	0	0	0	2	1	0	1	0	1	0	0	0	13	0	0	18	72.22
	B	0	0	0	4	2	0	0	4	0	0	0	0	0	6	2	18	33.33
	C	1	2	0	0	1	0	0	0	0	0	0	0	0	1	13	18	72.22

Table S8.4: Classification success (% correct) of CAP leave-one-out cross-validation for transects in Floreana.

9. DISTLM analysis

It should be noted that the amount of available variables to describe the water quality is often much larger than the amount of variables to describe the physical habitats. Hence, it makes sense that the number of variables included in any model would affect the results. Two-variable linear models for Floreana indicated that the physical habitat, represented by the cover of sand and bare rock, were most important to explain differences in fish assemblages, while for Santa Cruz water conditions, represented by temperature and Total P, were most important. However, down-scaling to one-variable models suggested that for both islands physical habitats were most useful to construct a parsimonious model. Hence, awareness regarding the representativeness of variables to represent specific aspects of the environment, i.e. water conditions or physical habitats, is key to interpret the data in a sound way.

In addition, measuring water quality is an objective procedure, while visually classifying physical habitats by providing an estimate of the cover of different artificial habitat classes is not. More difficult to describe or quantify aspects such as the characteristics of the algae cover (Chatfield et al., 2010), the structural complexities of the reef or the biomass of macrophytes (Young and Carr, 2015) may be important for specific species. Since we do not know how well the measured variables are representative for the actual environmental differences that fish sense, results should be handled with care. The models suggest that the main difference in physical habitats

	Variable series	Variable	pseudo-F	p-value	cum. R^2
Both islands	Water	Temperature	19.37	0.001	0.41
		Ammonium	8.10	0.001	0.55
		Phosphate	2.88	0.012	0.59
		Nitrite	3.16	0.007	0.64
		Sulfate	4.18	0.001	0.69
	Habitat	Vegetated rock	9.95	0.001	0.26
		Bare rock	7.87	0.002	0.43
		Rock with sediment deposition	4.33	0.005	0.51
	XY	Y	32.81	0.001	0.54
		X^3	5.17	0.001	0.61
Santa Cruz	Water	Total P	4.44	0.001	0.25
		Temperature	5.17	0.001	0.48
	Habitat	Rock with sediment deposition	4.91	0.001	0.27
	XY	Y^3	2.75	0.025	0.17
		X	3.69	0.006	0.37
		Y	5.31	0.004	0.57
Floreana	Water	Nitrite	1.56	0.189	0.11
	Habitat	Sand	3.94	0.004	0.23
		Bare rock	3.34	0.028	0.40
	XY	X^3	1.74	0.141	0.12

Table S9.1: Results of DISTLM analyses within series of predictors: water parameters (Water), physical habitats (Habitat) and geographical distances (XY). For both islands together (n=30) and separately (n=15).

sensed by fish in Santa Cruz is related to the observed difference in the type of rock cover, i.e. vegetation or sediment deposition, while for Floreana, the distinction between sand and rock cover is more important. Whether this rock is bare or covered by vegetation or sediment may not be of much importance. However, it may also be that the physical habitat was not observed by humans as it is sensed by fish and all constructed models based on these data may therefore be biased.

	No. Vars	AICc	R^2	Variable combination
Both islands	1	204.89	0.54	Y
	2	201.92	0.62	Sediment + X
	3	200.01	0.67	Sediment + X^3 + Temperature
	4	198.21	0.72	Veg + Sediment + Ammonium + X
	5	198.10	0.75	Veg + Sediment + Ammonium + X + Sand
	6	198.73	0.77	Veg + Sediment + Ammonium + X + Y + Sand
Santa Cruz	1	104.97	0.27	Sediment
	2	102.66	0.50	Sediment + Temperature
	3	103.45	0.59	Nitrate + Temperature + Ammonium
Floreana	1	94.966	0.23	Sand
	2	94.463	0.40	Sand + Bare
	3	94.463	0.40	Sand + Bare + Ammonium

Table S9.2: Results of DISTLM analyses for all predictors. All possible combinations of predictors and number of predictors were assessed without distinction between series of variables. Sediment, Sand and Veg refer to the cover of rock wit sediment deposition, sand and vegetated rock respectively.

	No. Vars	Series	Marginal tests			Sequential tests			
			pseudo-F	p-value	R^2	AICc	pseudo-F	p-value	cum. R^2
Both islands	4	XY	12.12	0.001	0.66	203.86	12.12	0.001	0.66
		Water	10.95	0.001	0.64	202.51	3.66	0.001	0.80
		Habitat	7.44	0.001	0.54	\	\	\	\
	2	XY	21.43	0.001	0.61	202.11	21.43	0.001	0.61
		Water	16.19	0.001	0,55	200.71	3.27	0.001	0.69
		Habitat	10.13	0.001	0.43	199.99	3.18	0.001	0.76
	1	XY	32.81	0.001	0.54	204.89	32.81	0.001	0.54
		Water	19.37	0.001	0.26	203.38	3.83	0.003	0.60
		Habitat	9.95	0.001	0.41	202.4	3.38	0.004	0.64
Santa Cruz	2	Water	5.52	0.001	0.48	103.17	5.52	0.001	0.48
		Habitat	4.05	0.001	0.40	\	\	\	\
		XY	3.51	0.003	0.37	\	\	\	\
	1	Habitat	4.92	0.001	0.27	104.97	4.91	0.001	0.27
		XY	2.74	0.022	0.17	104.48	3.33	0.011	0.43
		Water	4.44	0.002	0.25	\	\	\	\
Floreana	2	Habitat	4.00	0.001	0.40	92.28	4.00	0.001	0.40
		Water	2.22	0.034	0.27	\	\	\	\
		XY	1.35	0.208	0.18	\	\	\	\
	1	Habitat	3.94	0.003	0.23	94.97	3.94	0.007	0.23
		XY	1.74	0.153	0.11	\	\	\	\
		Water	1.56	0.189	0.12	\	\	\	\

Table S9.3: Results of DISTLM analyses using all predictors, without grouping them in different sets of variables.

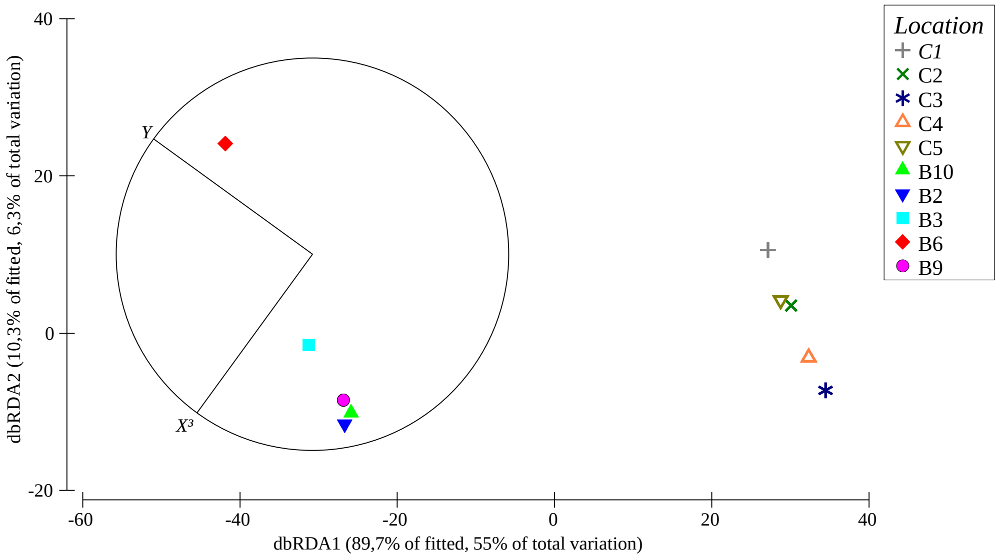

Figure S9.1: Constrained ordination of the fitted values of the most parsimonious DISTLM for all islands using series of variables (i.e. dbRDA). Since the most parsimonious model contained only one series (geographical distance) of which only two variables were retained (Y and X^3), only two dbRDA axes (linear combinations of PCO axes) were established. Hence both axes explained 100.0 % of the fitted variation. The axes explained 61.4 % of the total variation (i.e. 100 X R^2 (Table 3)). The length of each variable vector corresponds with the effect that variable had on the construction of the dbRDA axes.

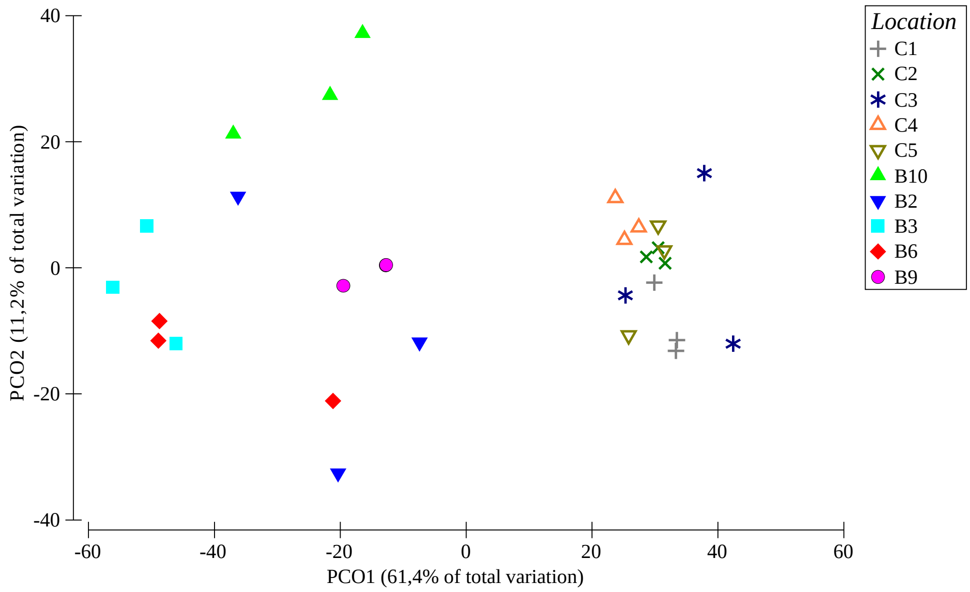

Figure S9.2: Unconstrained PCO ordination of the median-aggregated biological data for both islands.

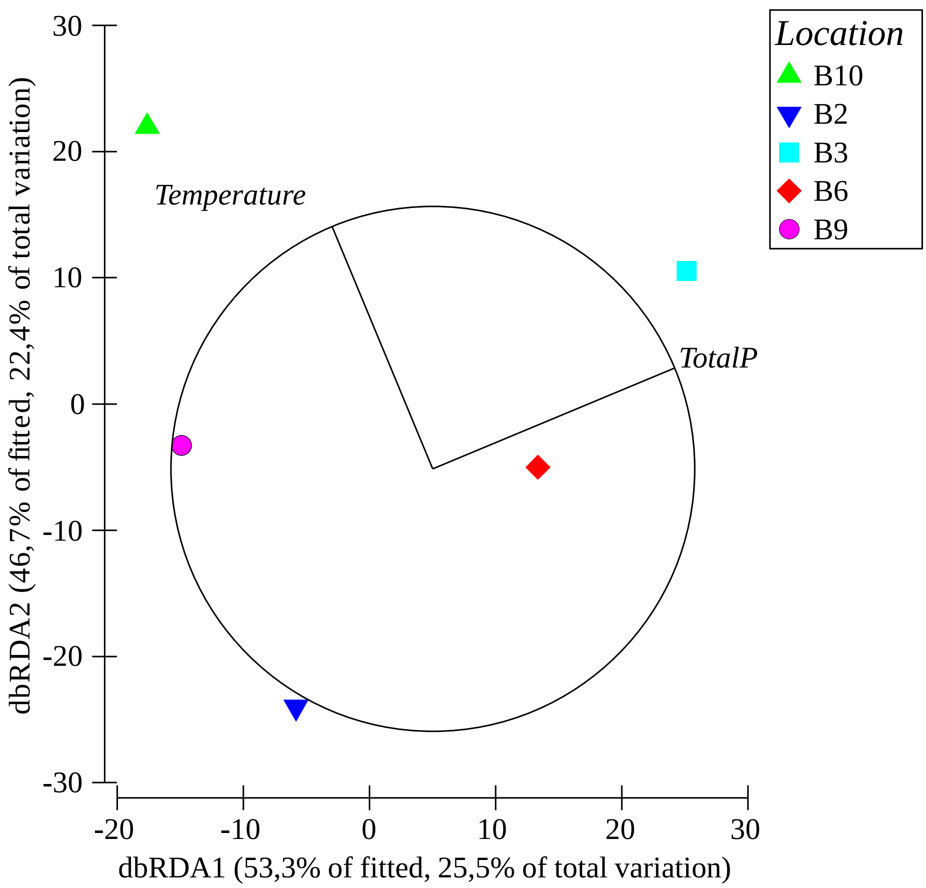

Figure S9.3: Constrained ordination of the fitted values of the most parsimonious DISTLM for Santa Cruz using series of variables (i.e. dbRDA). Since the most parsimonious model contained only one series (water conditions) of which only two variables were retained (Temperature and Total P), only two dbRDA axes (linear combinations of PCO axes) were established. Hence both axes explained 100.0 % of the fitted variation. The axes explained 47.9 % of the total variation (i.e. 100 X R^2 (Table 3)). The length of each variable vector corresponds with the effect that variable had on the construction of the dbRDA axes.

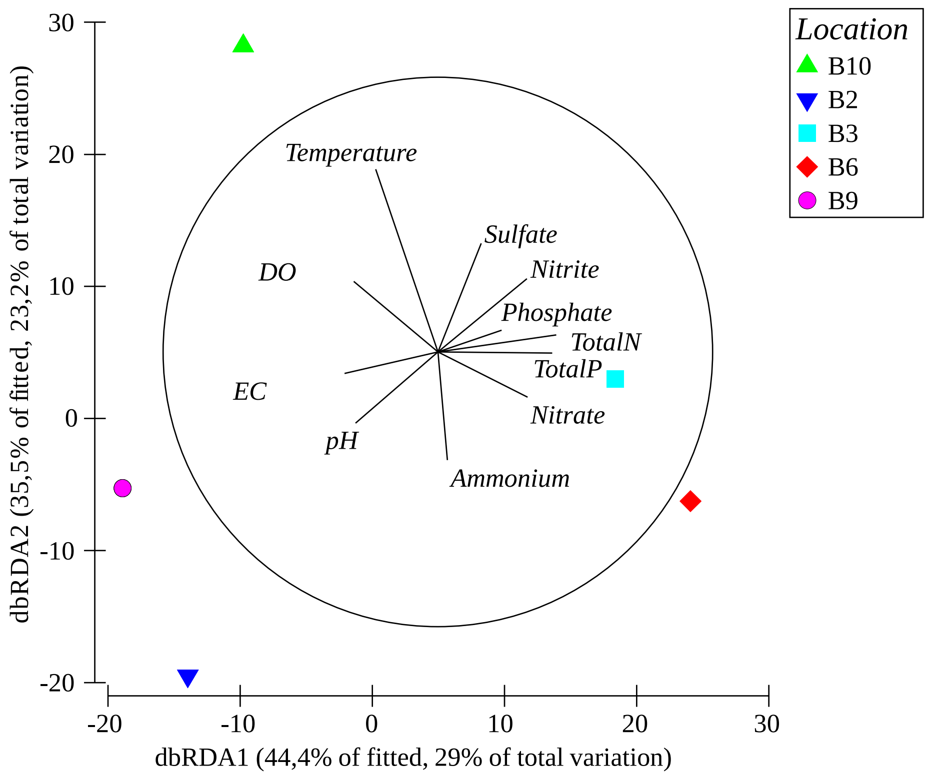

Figure S9.4: Constrained ordination of the fitted values of the DISTLM for Santa Cruz using all variables of the water conditions series (most explanatory series for Santa Cruz). Both axes explained 80.0 % of the fitted variation and 52.1 % of the total variation (i.e. 100 X R^2 (Table 3)). The length of each variable vector corresponds with the effect that variable had on the construction of the dbRDA axes.

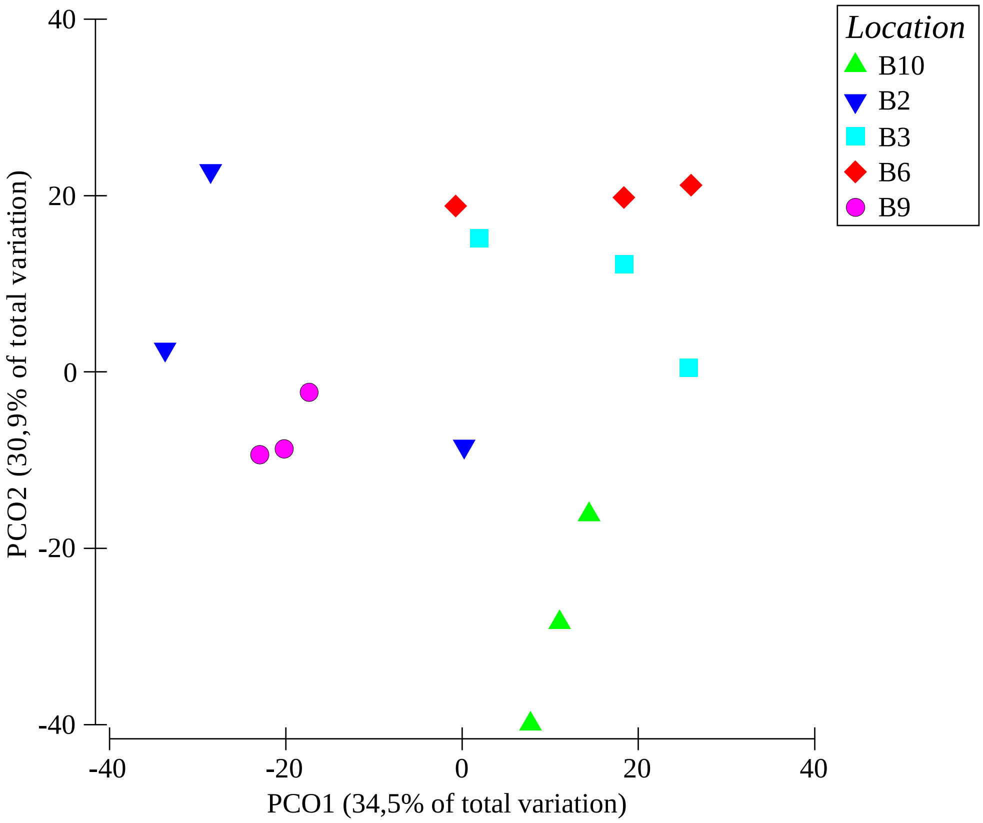

Figure S9.5: Unconstrained PCO ordination of the median-aggregated biological data for Santa Cruz.

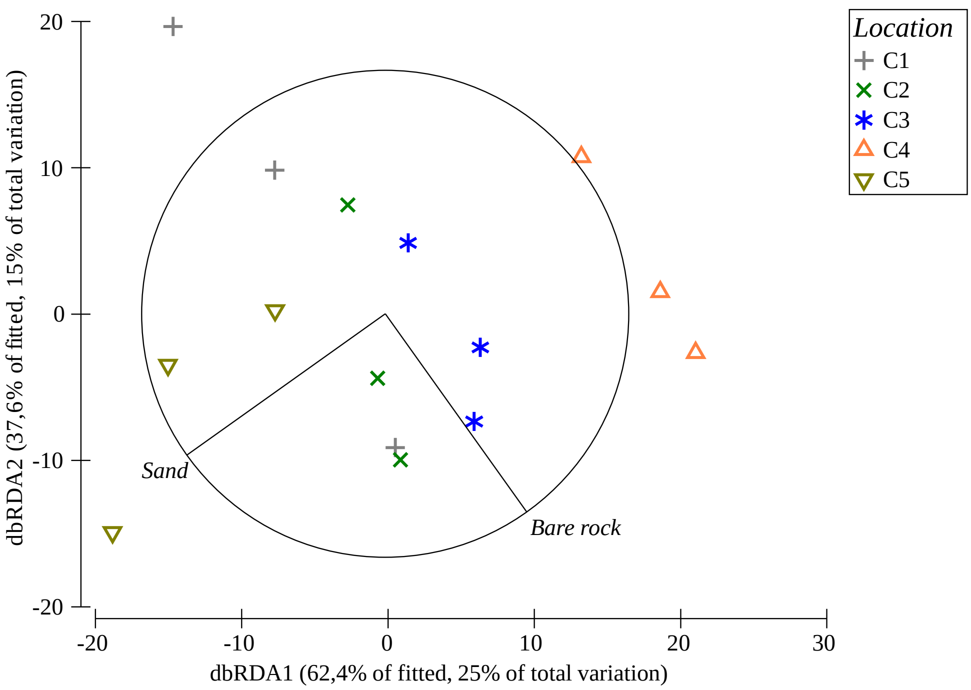

Figure S9.6: Constrained ordination of the fitted values of the most parsimonious DISTLM for Floreana using series of variables (i.e. dbRDA). Since the most parsimonious model contained only one series (physical habitat) of which only two variables were retained (percentage cover of sand and percentage cover of bare rock), only two dbRDA axes (linear combinations of PCO axes) were established. Hence both axes explained 100.0 % of the fitted variation. The axes explained 40.0 % of the total variation (i.e. 100 X R^2 (Table 3)). The length of each variable vector corresponds with the effect that variable had on the construction of the dbRDA axes.

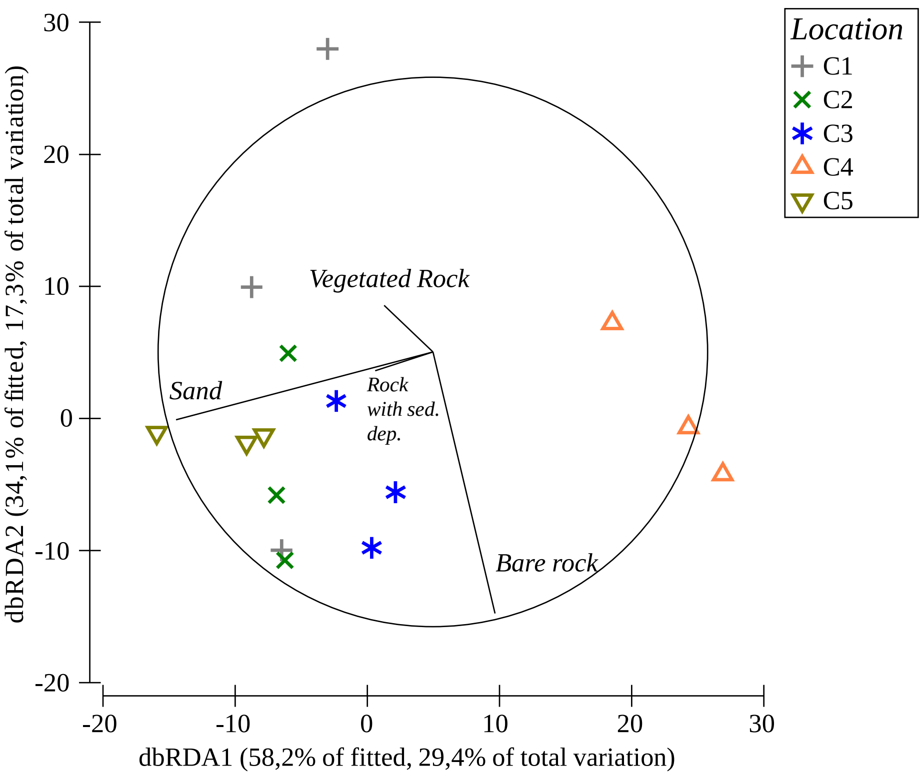

Figure S9.7: Constrained ordination of the fitted values of the DISTLM for Floreana using all variables of the physical habitats series (most explanatory series for Floreana). Both axes explained 92.3 % of the fitted variation and 46.7 % of the total variation (i.e. 100 X R^2 (Table 3)). The length of each variable vector corresponds with the effect that variable had on the construction of the dbRDA axes.

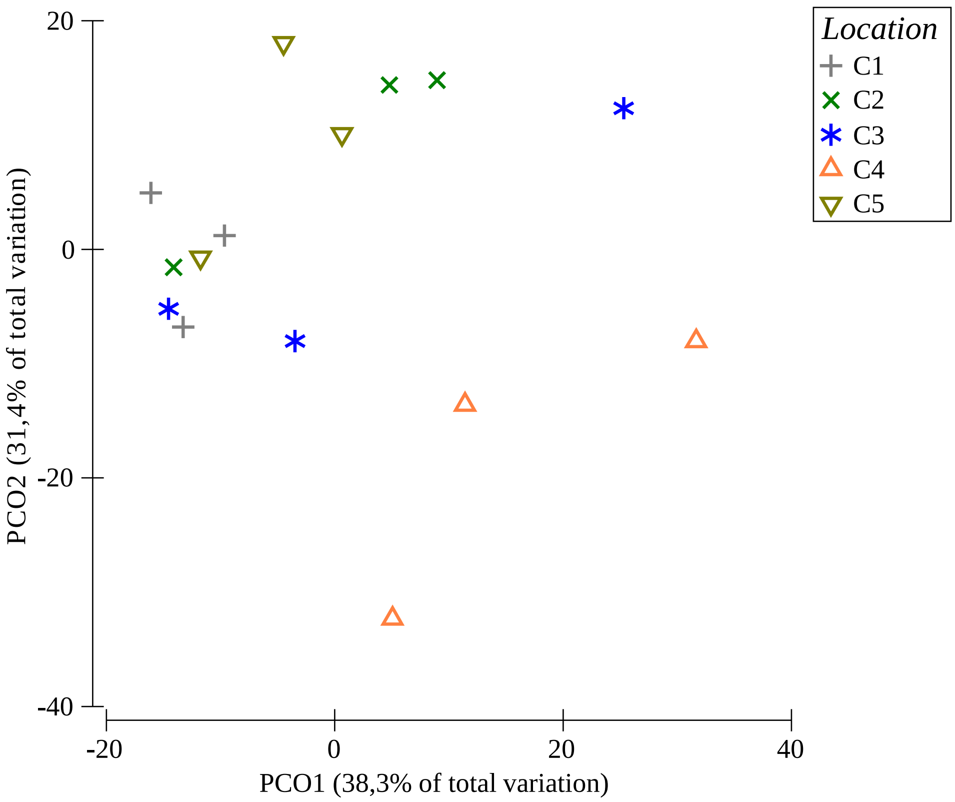

Figure S9.8: Unconstrained PCO ordination of the median-aggregated biological data for Floreana.

10. Comments statistical analyses

10.1. SACs

For each level of sampling effort, observations are resampled without replacement and the total number of different species over all considered observations per sampling event are counted. Finally, the average and confidence intervals of the 10^5 resampling events are determined for each level of sampling effort. The curvature provides insight in the expected species diversity (Chao and Shen, 2004)

10.2. β diversity

It should be noted that β diversity was also assessed with a PERMDISP analysis, as it can statistically be represented as the multivariate dispersion of the Sorensen resemblance dissimilarity matrix (presence/absence.) of the data. However, in this section, dispersion was determined to assess whether PERMANOVA-violations took place. Hence, data transformation and the type of dissimilarity matrix used were the same as those used for the corresponding PERMANOVA (i.e., Bray-Curtis resemblance matrix of the original fourth-root transformed data set). Throughout this work the term dispersion was used in the context of assessing any violations of model assumptions, while β diversity was used to refer to a specific type of multivariate dispersion with predetermined settings.

10.3. PERMANOVA

Because an asymptotically exact test was performed using a large number of permutations, it is reasonable to assume that the p-values and family-wise error rate (chance of at least one type I error (incorrect rejection of null hypothesis).) are not underestimated. Hence, with 10 comparisons and a 5% significance level, it would be expected that 0.5 rejections are due to chance (i.e., family-wise error rate). Since there were 5 significant rejections of the null hypothesis, it is unlikely that all of them were due to chance. The family-wise error rate hampers the exact identification of the real differences (as some of the differences might actually not be a difference) but does allow a relatively strong statement regarding the large number of significantly different locations within Santa Cruz, compared to within Floreana.

References

Chao, A., Shen, T. J., 2004. Nonparametric prediction in species sampling. Journal of Agricultural, Biological, and Environmental Statistics.

Chatfield, B. S., Van Niel, K. P., Kendrick, G. A., Harvey, E. S., 2010. Combining environmental gradients to explain and predict the structure of demersal fish distributions. Journal of Biogeography 37 (4), 593–605.

Chavez, F. P., Strutton, P. G., Friederich, G. E., Feely, R. A., Feldman, G. C., Foley, D. G., McPhaden, M. J., 1999. Biological and chemical response of the equatorial Pacific Ocean to the 1997-98 El Nino. Science 286 (5447), 2126–2131.

Cummings, J. A., Smedstad, O. M., 2013. Variational Data Assimilation for the Global Ocean. In: Ki Park, S., Liang, X. (Eds.), Data Assimilation for Atmospheric, Oceanic and Hydrologic Applications. Vol. II. Springer, Berlin, Ch. 13, pp. 303–343.

Edgar, G. J., Banks, S., Farina, J. M., Calvopina, M., Martinez, C., 2004. Regional biogeography of shallow reef fish and macro-invertebrate communities in the Galapagos archipelago. Journal of Biogeography 31 (7), 1107–1124.

Houvenaghel, G., 1978. Oceanographic Conditions in the Galapagos Archipelago and Their Relationships with Life on the Islands. In: Boje, R., Tomczak, M. (Eds.), Upwelling ecosystems. Springer, Berlin, pp. 181–200.

Legendre, P., Legendre, L., 2012. Numerical ecology, 3rd Edition. Elsevier.

Liu, Y., Xie, L., Morrison, J. M., Kamykowski, D., 2013. Dynamic downscaling of the impact of climate change on the ocean circulation in the Galápagos Archipelago. Advances in Meteorology.

Liu, Y., Xie, L., Morrison, J. M., Kamykowski, D., Sweet, W. V., 2014. Ocean Circulation and Water Mass Characteristics around the Galápagos Archipelago Simulated by a Multiscale Nested Ocean Circulation Model. International Journal of Oceanography.

Mateus, C., Guerrero, C. A., Quezada, G., Lara, D., Ochoa-Herrera, V., 2019. An integrated approach for evaluating water quality between 2007-2015 in Santa Cruz Island in the Galapagos Archipelago. Water 11 (5), 937.

NASA, 2019. Moderate-resolution Imaging Spectroradiometer (MODIS) Aqua Ocean Color Data.

NOAA, 2019. Cold and Warm Episodes by Season. https://origin.cpc.ncep.noaa.gov/. Date accessed: 2019-10-22.

Palacios, D. M., 2004. Seasonal patterns of sea-surface temperature and ocean color around the Galápagos: Regional and local influences. Deep-Sea Research Part II: Topical Studies in Oceanography 51 (1-3), 43–57.

Schaeffer, B. A., Morrison, J. M., Kamykowski, D., Feldman, G. C., Xie, L., Liu, Y., Sweet, W., McCulloch, A., Banks, S., 2008. Phytoplankton biomass distribution and identification of productive habitats within the Galapagos Marine Reserve by MODIS, a surface acquisition system, and in-situ measurements. Remote Sensing of Environment 112 (6), 3044–3054.

Werdeman, J. L., 2006. Effects of populated towns on water quality in neighboring Galàpagos bays. Tech. rep., University of Washington.

Young, M., Carr, M. H., 2015. Application of species distribution models to explain and predict the distribution, abundance and assemblage structure of nearshore temperate reef fishes. Diversity and Distributions 21 (12), 1428–1440.